# X-ray Scattering Using Synchrotron Radiation Shows Nitrite Reductase from *Achromobacter xylosoxidans* To Be a Trimer in Solution†

J. Günter Grossmann,‡,§ Zelda H. L. Abraham,∥ Elinor T. Adman,⊥ Margarete Neu,‡ Robert R. Eady,∥ Barry E. Smith,∥ and S. Samar Hasnain*,‡

*Molecular Biophysics Group, SERC Daresbury Laboratory, Warrington WA4 4AD, Cheshire, U.K., AFRC IPSR Nitrogen Fixation Laboratory, University of Sussex, Brighton BN1 9RQ, U.K., Department of Biological Structure, University of Washington, Seattle, Washington 98195, and Institut für Genetik und für Toxikologie von Spaltstoffen, Kernforschungzentrum Karlsruhe, Postfach 3640, DW-7500 Karlsruhe, Germany*

*Received January 20, 1993; Revised Manuscript Received May 10, 1993*

ABSTRACT: We demonstrate here the applicability of X-ray scattering for studying molecular conformation of multimeric proteins in solution by using synchrotron radiation to extend the range of data collection to include medium angles (ca. 3–4°). We have been able to define the solution structure of the dissimilatory nitrite reductase of *Achromobacter xylosoxidans* (AxNiR), an enzyme for which there are conflicting reports as to the nature of its multimeric structure. Quantitative interpretation of the X-ray scattering profile, based on a modeling study using the high-resolution crystal structure data for the nitrite reductase from the related organism *Achromobacter cycloclastes* (AcNiR), provides a detailed model for the trimeric structure of AxNiR in solution. Sedimentation equilibrium centrifugation gave an $M_r$ of 103 000, consistent with such a trimeric structure.

The assignment of the three-dimensional structure of large multimeric proteins is often hindered by the lack of suitable crystals for X-ray diffraction structure analysis. The availability of monochromatic X-rays from synchroton radiation sources has recently enabled X-ray scattering of proteins in solution to be applied to this problem. Although an X-ray scattering pattern provides information at a lower resolution than X-ray diffraction, due to the orientational averaging that occurs in solution, the overall molecular conformation can be explored. When the experimental scattering profile of a protein is simulated using models based on its crystallographic structure coordinates, major insights can be obtained into its solution structure. In addition, conformational changes associated with the binding of small molecules to the protein can be defined in some detail with some confidence. This approach has recently been successfully used by us to model changes in the conformation of transferrin which occur when Fe and other metals bind to the metal binding site of this protein (Grossmann et al., 1992, 1993).

Dissimilatory nitrite reductase is the key enzyme in the anaerobic respiratory pathway by which denitrifying bacteria reduce nitrate to the gaseous products NO, $N_2O$, and $N_2$, since it is at this point in the denitrification pathway that significant losses of fixed nitrogen from the soil to the atmosphere occur. Dissimilatory nitrite reductases (NiR) have been purified from a number of organisms, and it is clear that there are two classes of enzymes, one containing diheme (heme $cd_1$) and the other copper as the redox active centers [see Hochstein and Tomlinson (1989)].

The $cd_1$ heme-containing enzymes, when isolated from a variety of denitrifying organisms, form a group with very similar physicochemical properties. In contrast, copper-containing NiRs show considerable structural diversity, with apparent variation in their native molecular weight (69 000–110 000), number of subunits (2–4), and number (2–4) and type of copper center (1 or 2) that they contain [see Denariaz et al. (1991)]. This variation is surprising, since this class of enzymes often shows antigenic cross reactivity (Coyne et al., 1989).

Of the copper-containing enzymes, the enzyme from the *Achromobacter cycloclastes* (AcNiR) has been studied extensively. This enzyme was considered on the basis of gel filtration (Iwasaki & Matsubara, 1972) and sedimentation equilibrium centrifugation (Liu et al., 1986) analyses to have a native $M_r$ of 69 000 with two subunits of 37 000. The copper atoms are present in two different ligand environments and are distinguishable by their electron paramagnetic resonance (EPR) spectra (Iwasaki & Matsubara, 1972). The recent X-ray crystallographic structure determination of AcNiR showed surprisingly that this enzyme is trimeric, in contrast with all earlier studies. A reinvestigation of the solution structure by sedimentation equilibrium centrifugation supported the crystallographic interpretation (Godden et al., 1991). The crystal structure also indicated the position of both types of copper sites, with the type 1 Cu site buried in each of the subunits while the type 2 Cu sites are at the subunit interface with ligation provided by both subunits.

Purified NiR from the closely related organism *Achromobacter xylosoxidans* (AxNiR), has variously been reported to be a dimer ($M_r$ ~70 000) as determined by gel filtration analysis (Masuko et al., 1984) or considerably larger ($M_r$ ~149 000) as determined by sedimentation velocity centrifugation (Iwasaki et al., 1963). This enzyme has also been reported to contain only type 1 copper (Masuko et al., 1984), but we have recently obtained preparations of 10-fold higher activity which have EPR spectra consistent with the presence of both type 1 and type 2 copper (Abraham et al., 1992). The properties of our preparations of AxNiR are very similar to those of AcNiR, although there are significant differences in the visible spectra, which result in the former enzyme being blue in solution and the latter green.

† SERC, AFRC, and KfK are thanked for financial support. Partial support from GM31770 (ETA) is also acknowledged.

* To whom correspondence should be addressed.
‡ SERC Daresbury Laboratory.
§ Kernforschungzentrum Karlsruhe.
∥ University of Sussex.
⊥ University of Washington.

0006-2960/93/0432-7360$04.00/0 

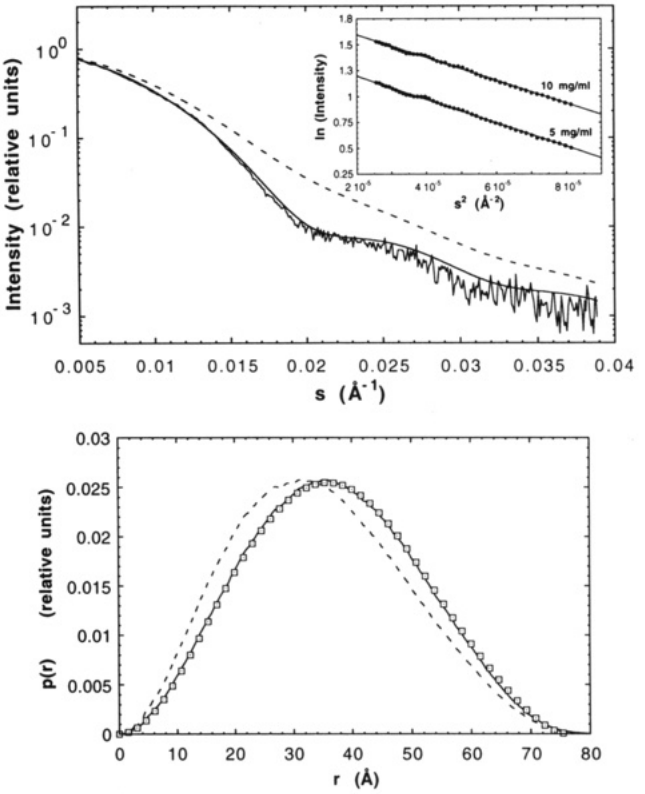


FIGURE 1: (a, top) Experimental scattering pattern for NiR (5 mg/mL) compared to profiles for a dimeric and a trimeric association based on crystal structure information (see text). The profiles computed for the crystal structure of a dimer (- - -) and a trimer (—) as well as the experimental curve were normalized to unity at zero scattering angle. The inset shows the Guinier plot for both concentrations from which the $R_g$ values were derived. (b, bottom) Distance distribution functions $p(r)$ calculated for a dimer (- - -) and a trimer (—) on the basis of the crystal structure of AcNiR (Godden et al., 1991) and from the experimental data at a concentration of 5 mg/mL (⊡). The size of the symbol is equal to the error in $p(r)$. For reasons of smoothness the theoretical $p(r)$ functions were calculated with a bin size of 0.5 Å. The comparison was achieved by normalizing the area under each curve to unity.

Table I: Radius of Gyration ($R_g$) Determined by Solution X-ray Scattering Measurements and Calculated from Model Structures[a]

| | | $R_g$ (Å), Guinier | $R_g$ (Å), $p(r)$ |
|---|---|---|---|
| | Experiment | | |
| | 5 mg/mL soln | 28.7 (0.5) | 28.0 (0.2) |
| | 10 mg/mL soln | 28.3 (0.3) | 27.7 (0.2) |
| | Simulation | | |
| dimer | crystal structure | 26.5 | 26.2 |
| trimer | crystal structure | 28.3 | 27.8[b] |
| | hydrated structure | 28.6 | 28.2[b] |

[a] The experimental errors are shown in parentheses. All values were computed according to eqs 1 and 2. The values determined from the Guinier plot ($0.005\ Å^{-1} < s < 0.009\ Å^{-1}$) are somewhat larger than those obtained by the $p(r)$ analysis. This is possible because the latter procedure uses the whole information content of the scattering profile ($s \leq 0.038$ Å$^{-1}$), whereas the Guinier approximation is restricted to a small range (the innermost part of the scattering curve) which is not completely available due to the beam stop. The inevitable beam stop protects the detector against radiation damage. [b] The same values were computed from the crystallographic atomic coordinates through use of the formula $R_g^2 = \sum_i z_i R_i^2 / \sum_i z_i$, where $z_i$ is the electronic charge of atom $i$ at the distance $R_i$ from the electronic center of mass.

The number of subunits in NiR from different organisms and their spatial organization are essential to an understanding of the role(s) of the two types of copper centers which are present in both enzymes, since in AcNiR the copper binding site for type 2 copper is formed at the subunit interface. Indeed,

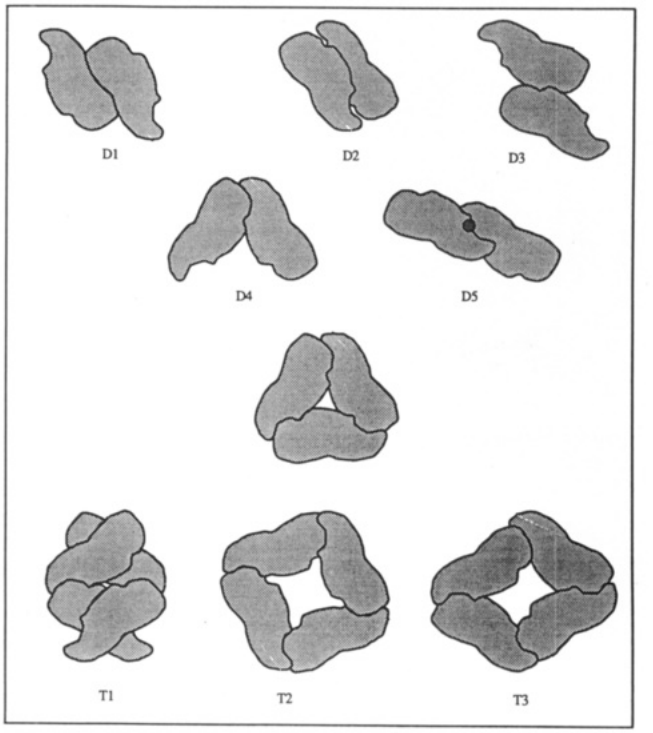


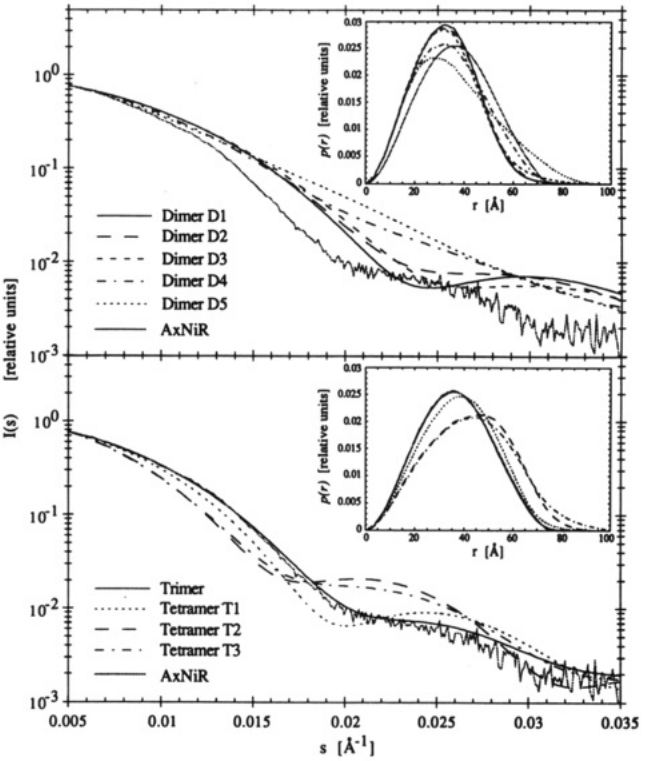


FIGURE 2: (a, top) Schematic representation of subunit arrangements for a variety of dimeric (D1–D5) and tetrameric (T1–T3) models for AxNiR. The dimer D4 is obtained by taking away a monomer of the AcNiR crystallographic model (shown in the center of the figure) and has been used as a template for tetramers T1 and T3. $R_g$ values for D1 and D2 are 24.7 Å, while D3, D4, and D5 have values of 25.3, 26.2, and 28.5 Å, respectively. T1, T2, and T3 have $R_g$ values of 29.2, 32.2, and 33.2 Å. (b, bottom) Comparison of the calculated scattering curve $I(s)$ and the distance distribution function $p(r)$, obtained using model shown in (a), with the experimental curves. The $I(s)$ profiles are normalized at $s = 0.005$ Å$^{-1}$ with respect to AxNiR. Plots for $p(r)$ functions are normalized to a unit area. This has been done to show the qualitative changes.

the specific activity of NiR has been shown to correlate with the amount of type 2 copper present (Libby & Averill, 1992).

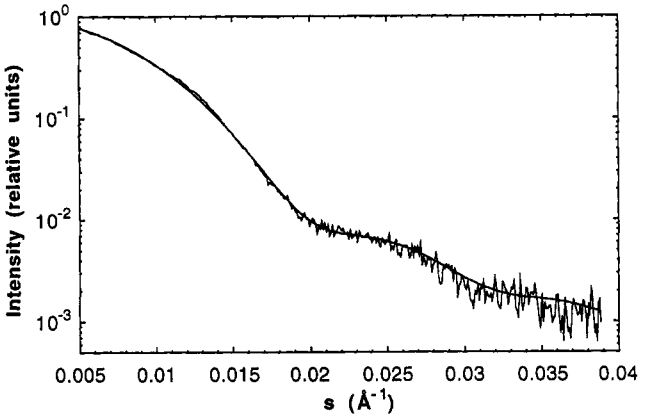


FIGURE 3: Scattering profile of the NiR trimer including a solvent layer of 716 water oxygens compared with the experimental result (5 mg/mL).

We report in the present paper the use of synchrotron radiation small-angle X-ray scattering (SRXS) which in conjunction with the coordinates of the crystal structure of AcNiR has allowed us to model the solution structure of AxNiR. The trimeric structure derived from our analysis is supported by our sedimentation equilibrium ultracentrifugation studies but conflicts with gel filtration data also reported below. These data, and the crystallographic and ultracentrifugation data obtained by Godden et al. (1991) for the closely related enzyme AcNiR, are discussed.

## MATERIALS AND METHODS

*Purification of Enzyme.* The dissimilatory nitrite reductase of *A. xylosoxidans* (NCIMB 11015; also named *Alcaligenes xylosoxidans*; previously *Alcaligenes sp.* NCIMB 11015/*Pseudomonas denitrificans*) was isolated from cells grown anaerobically with nitrite as the terminal electron acceptor. Nitrite reductase was purified to homogeneity on SDS–PAGE by a combination of ammonium sulfate fractionation and ion-exchange chromatography (Abraham et al., 1993). The purified enzyme had a specific activity of 150 $\mu$M $NO_2^-$ reduced $min^{-1}$ (mg of protein)$^{-1}$ when assayed at 25 °C using methyl viologen reduced with an excess of dithionite as the electron donor, as described previously for the assay of nitrate reductase, except that nitrite (0.1 mM) was substituted for nitrate (MacGregor, 1978). Dithiothreitol was omitted from the assay mixture since in its presence the nonenzymic reduction of nitrite has been reported under these conditions (Farnden & Robertson, 1980).

*X-ray Scattering Measurements.* Data were recorded on the X-ray scattering station 8.2 at the Daresbury Synchrotron Radiation Source, Daresbury, U.K. (Gerritsen & Robertus, 1990). An X-ray wavelength of 1.5 Å was used with a sample to detector separation of 3 m. Scattered X-rays were recorded in the range $0.005\ Å^{-1} \leq s \leq 0.038\ Å^{-1}$ on a position-sensitive proportional counter (quadrant detector) with an associated data acquisition system (Lewis et al., 1988). The scattering parameter $s$ is defined by $s = (2 \sin \theta)/\lambda$, where $2\theta$ is the scattering angle. Individual samples were exposed to X-rays for no longer than 15 min, and scattering curves were recorded in 3-min time frames so as to check for potential radiation damage or aggregation of material on the window, as well as to establish the reproducibility of data obtained in repeated measurements. The total measuring time was 150 and 30 min for concentrations of 5 and 10 mg/mL AxNiR, respectively. In order to minimize errors due to the subtraction of background and instrument function, measurements of buffer (50 mM phosphate, pH 7.2, containing 50 mM NaCl) and sample were made alternatively for equal times. All measurements were made at room temperature (22–24 °C). Data treatment including correction for the beam decay and detector response as well as background subtraction followed the analysis procedure which was described recently in detail (Grossmann et al., 1992, 1993). Furthermore, the interpretation of the intensity profiles involved the determination of the intramolecular distances or the distance distribution function $p(r)$. The scattering patterns were analyzed with the program GNOM (Semenyuk & Svergun, 1991), which searches for $p(r)$ in order to fit the experimental conditions and error bounds. This procedure uses an indirect transform method, based on the regularization technique (Svergun et al., 1988).

*Ultracentrifugation.* Low-speed sedimentation equilibrium centrifugation was carried out at 20 °C and 14 000 revolutions/min using a Beckmann XL-A analytical ultracentrifuge using absorption optics at 277 nm. Equilibrium was considered to have been established when two consecutive scans, recorded several hours apart, appeared identical. The final solute distribution was analyzed using the FORTRAN MSTARA program. Whole-cell weight-averaged molecular weights ($M_{0w}$) were extracted using the limiting value at the cell base of the $M^*$ (point-averaged molecular weight) function (Harding et al., 1992). Samples of nitrite reductase were dialyzed overnight against 150 mM Tris-HCl buffer, pH 7.5, or 50 mM phosphate buffer, pH 7.2, containing 50 mM NaCl, and the dialysis buffer was used in the experiments as a cell blank. A partial specific volume of 0.7435 was calculated from the amino acid composition (Abraham et al., 1993).

*Molecular Weight Determination by Gel Filtration.* A Pharmacia FPLC system was employed to determine the relative $M_r$ of nitrite reductase using a Superose-12 column (30 cm × 1 cm). The column was calibrated with the following standard proteins: cytochrome *c* (12 400), carbonic anhydrase (29 000), ovalbumin (45 000), bovine serum albumin (66 000), alcohol dehydrogenase (150 000), and $\beta$-amylase (200 000), which were obtained as a molecular weight standard kit from Sigma. The column was equilibrated with 50 mM phosphate buffer, pH 7.2, containing 50 mM NaCl with or without 10% ethanediol, or 50 mM Tris-HCl buffer, pH 7.6, containing 50 mM NaCl. The sample volume was 50 or 100 $\mu$L, and both the buffer flow rate and concentrtion of protein loaded were varied as indicated.

## RESULTS AND DISCUSSION

*Gel Filtration.* Calibration curves for the native $M_r$ of AxNir were determined by gel filtration on Superose-12. A single symmetrical peak of AxNir was observed over a range of initial loading protein concentrations from 0.4 to 24 mg/mL, and the retention volume did not change significantly (12.66 ± 0.03 mL) over this range of protein concentrations. The absence of any effect of protein concentration on the retention volume and peak shape suggests that protein association–dissociation was not occurring to any significant extent under these conditions. The $M_r$ evaluated from calibrated columns run under a variety of buffer flow rates (0.1–0.5 mL/min) with either phosphate buffer or Tris-HCl buffer also gave consistent retention volumes for AxNiR, indicating that slow association–dissociation was not occurring and gave an average value of 75 000 ± 3500 for the native $M_r$.

These data, together with the subunit molecular weight data of 36 800 ± 600 determined by SDS–PAGE and 36 523

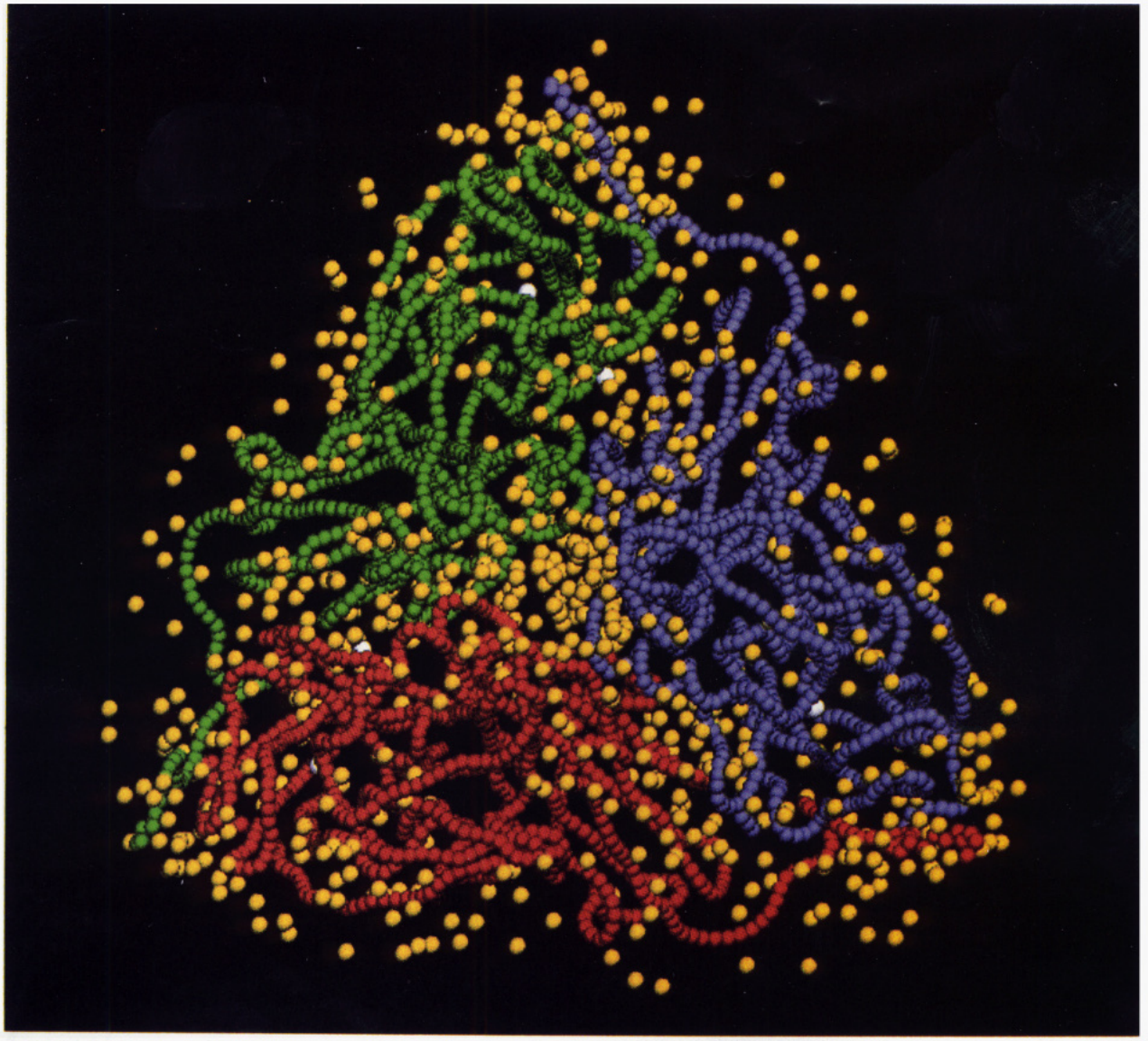

FIGURE 4: A model of the hydrated trimer of NiR used for the scattering pattern simulation as shown in Figure 3. In order to illustrate the trimeric association, the monomers are represented by their smoothed backbone structures using different colors (red, green, and blue). Water oxygens are shown as yellow spheres. The copper atoms are shown as white spheres.

± 9.8 from electrospray mass spectrometry (Abraham et al., 1993), suggest that, under the conditions used in the gel filtration experiments, AxNiR is a dimer in solution. On the basis of SDS–PAGE and gel filtration experiments other workers have also reported AxNiR to be a dimer of two identical subunits (Iwasaki, 1976; Masuko et al., 1984). Using the same combination of techniques, the NiR of *A. cycloclastes* was also considered to be a dimeric protein (Liu et al., 1986) until surprisingly the X-ray crystallographic structure showed it to be a trimer, a model which was supported by sedimentation equilibrium data (Godden et al., 1991).

*X-ray Scattering Measurements.* Since no suitable crystals of NiR from *A. xylosoxidans* are available at present for X-ray structure analysis, we applied the solution X-ray scattering technique to AxNiR in order to obtain some direct structural information about its molecular arrangement. In contrast to X-ray crystallography, an X-ray scattering profile provides information at low to medium resolution due to the orientational averaging that takes place in the noncrystalline material (Glatter, 1982; Feigin & Severgun, 1987). However, when combined with high-resolution crystallographic parameters, an unambiguous interpretation of SRXS profiles is possible and allows one to explore molecular conformations under almost physiological conditions. This approach is very powerful, and in the present case the multimeric solution structure of NiR could be compared with the crystallographic findings.

Synchrotron X-rays were used for the solution scattering experiments, which were performed with sample concentrations of 5 and 10 mg/mL. Careful inspection of the recorded time frames showed no differences in the scattering behavior, which indicates the stability of the enzyme against the exposure of high-intensity X-rays. Figure 1a presents the averaged and complete experimental scattering profile for 5 mg/mL (the profile for 10 mg/mL revealed the same features and is therefore not shown). The monodispersity of the particles in solution is also given according to the linearity in the low-angle range as seen in the Guinier plot (inset of Figure 1a). The Guinier approximation (Guinier, 1939) holds for sufficiently small scattering angles, and when ln $I(s)$ is plotted versus $s^2$, the radius of gyration, $R_g$, can be calculated from the slope $m$

$$R_g^2 = -3m/4\pi^2 \quad (1)$$

Another method to evaluate this structural parameter follows

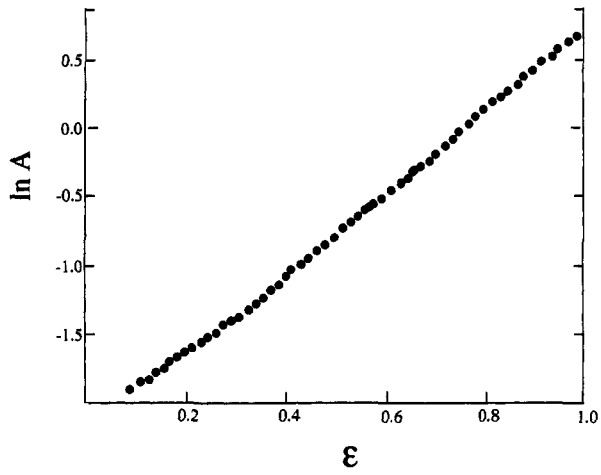


FIGURE 5: Plot of ln absorbance at 277 nm vs $\epsilon$, the normalized radial displacement parameter [$\epsilon = (r^2 - a^2)/(b^2 - a^2)$], where $r$ is the radial displacement and $a$ and $b$ are the corresponding values at the cell meniscus and base, respectively. The protein concentration was initially 0.5 mg/mL in 50 mM Tris-HCl buffer, pH 7.5; similar results were obtained in 50 mM phosphate buffer, pH 7.2, containing 50 mM NaCl.

the indirect transformation procedure (Svergun et al., 1988) which uses the entire scattering profile and yields the distance distribution function $p(r)$

$$R_g^2 = \frac{\int_0^D r^2 p(r)\, dr}{2\int_0^D p(r)\, dr} \qquad (2)$$

The $p(r)$ function represents the distribution of all intramolecular distances between two scattering centers (atoms) and is 0 for $r > D$, where $D$ is the maximum size of the molecule. The experimental $R_g$ values given in Table I indicate that the concentration dependence of $R_g$ is not significant.

*Simulation of Scattering Profiles.* The reversed procedure was applied in order to simulate the scattering profiles using models based on the crystallographic coordinates of AcNiR (Godden et al., 1991). The distance distribution can be calculated from crystal structures using all non-hydrogen coordinates. For this, distances between every pair of atoms were binned (bin size 0.1 Å) and weighted according to the product of the number of electrons, thus resulting in a histogram $p(r_i)$. The computation of the scattering curve was done with formula

$$I(s) = g(s)\sum_i p(r_i)\, \sin(2\pi s r_i)/(2\pi s r_i) \qquad (3)$$

where the summation extends from $r_i = 0$ to $r_i = D$. Since a molecule is represented by a volume with a certain shape, each scattering centre (given by its atomic coordinates) is associated with a geometrical volume which is introduced mathematically by a shape factor $g(s)$ (Rolbin et al., 1974). Spheres with a radius of 1.7 Å were used. The sphere dimension approximately correlates with the average van der Waals radius of non-hydrogen atoms in proteins.

In Figure 1a we present two scattering profiles computed from the dimeric and the trimeric models for the protein using 5152 and 7728 non-hydrogen atoms for the dimer and trimer, respectively. The structural parameters for a dimeric and trimeric arrangement of the molecule are also given in Table I. It is clear that the dimeric model does not adequately represent the NiR molecule in solution at the concentrations used. This result is further supported by the data in Figure 1b in which $p(r)$ calculated using the dimeric and trimeric models is compared with the solution X-ray scattering data.

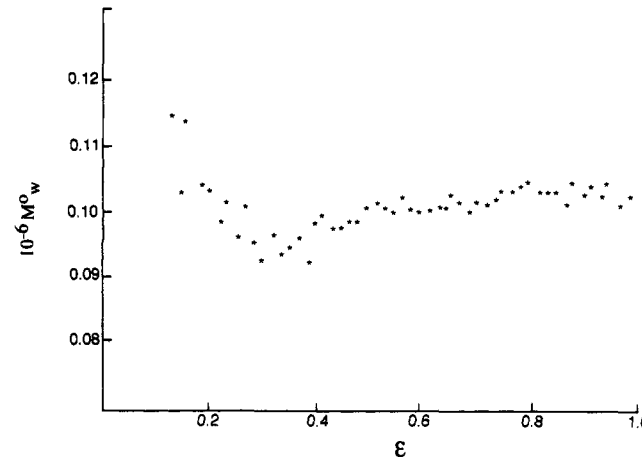


FIGURE 6: Plot of the whole-cell weight-averaged $M_r$ for AxNiR as a function of $\epsilon$ from the data of Figure 5.

The dimer was initially generated by taking one monomer away from the trimeric structure. Several alternative dimeric arrangements were modeled, e.g., the distance between the two monomers was varied, but these did not fit the striking characteristics (e.g., the amplitude and periodicity of oscillation in the scattering pattern) of the experimental pattern. In addition, a number of tetrameric structures were constructed using the molecular envelope of the monomer. Some of these models and their corresponding scattering curves along with their $R_g$ values are shown in panels a and b of Figure 2, respectively. The structural basis of model building was mainly geometric and included symmetry considerations as well as distance constraints. The latter were derived from the $p(r)$ function of the experimental scattering data. In the case of dimeric association, a large interface between the monomers was ensured in order to exclude solvent. The chemical nature of the molecular surface and, in particular, the maintenance of the type 2 Cu site (at the monomer–monomer interface) have not been taken into account. This has been partly done to explore the significantly different configuration for AxNiR compared to AcNiR's crystallographic structure. It is clear from Figures 1 and 2 that only the trimeric model mimics the solution scattering data in a satisfactory manner. It is worth noting that even though $R_g$ values for some of the dimeric and tetrameric models are very similar to the experimental value, the characteristics of the observed scattering pattern are not reproduced by any of these models. This illustrates the importance of obtaining high-quality data to medium angles (4°) and for simulating the scattering pattern over the widest range possible. It is the characteristic structural features in the scattering pattern which provide a clear distinction (see Figures 1 and 2) between different oligomeric arrangements. We note that similar differences in the scattering curves for dimeric, tetrameric, and octameric models were shown for pyruvate decarboxylase (Konig et al., 1992), for which no atomic structure is yet known.

The simulation of the scattering curve could be improved significantly (Figure 3) by incorporating a hydration layer (Figure 4) surrounding the trimeric structure. The significant improvement observed for the majority of the scattering range $s \geq 0.015$ Å$^{-1}$, compared to Figure 1a, provides further confidence to the interpretation of the scattering data. Although these water molecules are not yet accessible crystallographically, we used an energy minimization procedure to estimate the amount of hydration. In this approach a solvation shell of water molecules was constructed around the crystallographic structure of the trimer. First, the solvent

molecules were placed on a diamond-shaped grid built around the structure extending over about 6 Å from the molecular surface. This was achieved with the molecular graphics program BIOGRAF (version 2.0, BioDesign, Inc., Sunnyvale, CA). Since the location and orientation of the water molecules are still arbitrary, the determination of an optimal structure was attained by minimizing the energy of the whole geometry. The energy minimization computations were carried out in an iterative manner with the program X-PLOR (version 2.1 by A. T. Brünger, Yale University, New Haven, CT). In order to find the best agreement between experimental and simulated scattering profiles, water oxygens within a certain range from the protein surface were included into the calculations. The best fit to the data yielded a solvent shell of 716 water oxygens up to a maximum distance of 3.15 Å from the surface. This result can be associated with a hydration of approximately 0.12 g of $H_2O$/g of protein and gives an estimate of the water content of NiR. However, this rather small solvent contribution compared to 0.38 g of $H_2O$/g of protein corresponding to a full hydration (Rupley et al., 1983) can only be considered as the amount of tightly bound water representing a permanent part of the trimer framework. It is this water shell very close to the surface which is different from bulk water and thus contributes to the X-ray scattering. A relatively conservative estimate of the total number of waters expected to be found in the crystal structure is one per residue, which here would be 340 × 3 or 1020.

Thus the trimer structure as revealed by the crystallographic structure for AcNiR is fully consistent with the solution scattering data of AxNiR, at least for the concentrations used here. On this basis, the NiRs from both *A. cycloclastes* and *A. xylosoxidans* appear to have more similarities in terms of their solution properties and redox centers than previously thought.

*Ultracentrifugation.* Because of the discrepancy of $M_r$ determined by gel filtration and X-ray scattering, we also used ultracentrifugation techniques to obtain additional information at significantly lower concentration. Sedimentation velocity analysis of AxNiR at 4.5 mg/mL in 50 mM Tris-HCl buffer at pH 7 showed a single symmetrical boundary (consistent with our preparations of AxNiR being monodisperse) throughout sedimentation, and analysis gave a value for the sedimentation coefficient of 6.3 S. In low-speed sedimentation equilibrium experiments the plot of log absorbance (i.e., AxNiR concentration) vs the square of the radial distance was essentially linear (Figure 5), indicating that the sample exhibited only very slight heterogeneity. Whole-cell weight-averaged molecular weights ($M_{0w}$) were extracted by using the limiting value at the cell base of the $M^*$ (point-averaged molecular weight) function and gave a value of 103 000 ± 5000 (Figure 6). This value clearly indicates that the trimer is the predominant species present under these conditions. Similar conclusions were drawn by Godden et al. (1991) from a sedimentation equilibrium study of AxNiR, but in this system significant dissociation was observed at protein concentrations below 0.2 mg/mL, with monomer–trimer or monomer–dimer–trimer equilibria giving equally good fits to the data.

*Concluding Remarks.* The crystal structure of AcNiR has revealed that type 2 copper is bound at the interface of the monomeric subunits within the trimeric structure (Godden et al., 1991). Clearly, retention of the trimeric structure (or minimally a dimeric structure) is necessary to maintain the relative orientation of the two domains which bind the copper atom. The finding reported here, that AxNiR is also a trimer and contains both type 1 and type 2 copper (Abraham et al., 1993), strongly suggests that a similar interface will be found in this molecule, but further structural work will be necessary to confirm this.

A trimeric structure for proteins is no longer as unusual as it once seemed: two recently determined X-ray structures of unrelated proteins have shown that not only are they trimeric structures but they also exhibit a long arm extending from one monomer to another monomer in the trimer (Cedergren-Zeppezauer et al., 1992; Mattevi et al., 1992). This feature can be seen in AcNiR (Godden et al., 1991) and AxNiR (see Figure 4).

The current work on AxNiR and data for AcNiR indicate that these proteins behave anomalously on gel filtration and give a misleading impression of their oligomeric solution structure. Sedimentation equilibrium ultracentrifugation measurements gave results for the molecular weight consistent with X-ray scattering data and thus perhaps should be used wherever possible when characterizing a new oligomeric protein.

Our X-ray scattering data demonstrate that it is a powerful tool for determining solution structures of proteins, particularly when applied in concert with other structural techniques. In addition, the availability of intense collimating X-ray beams from a synchrotron radiation source enables the collection of data within short time scales and with significant statistics extending to high scattering angles where subdomain (Grossmann et al., 1992, 1993) and multimeric arrangements in proteins can be detected with confidence. The quantitative approach adopted here provides considerable detail of the organization of the monomeric units in an oligomeric structure.

## ACKNOWLEDGMENT

We are grateful to Dr. Svergun, who provided the latest version of the GNOM program. The encouragement and help of Professor H. Appel is much appreciated. We also acknowledge Les Sarco at the School of Biological Sciences, University of Sussex, and Drs. S. E. Harding and P. J. Morgan of National Hydrodynamics Institute, University of Nottingham, for providing their technical expertise and ultracentrifugation facilities.

## REFERENCES

Abraham, Z., Lowe, D. J., & Smith, B. E. (1993) *Biochem. J.* (submitted for publication).

Cedergren-Zeppezauer, E. S., Larsson, G., Nyman, P. O., Dauter, Z., & Wilson, K. S. (1992) *Nature 355*, 740–743.

Coyne, M. S., Arunakumari, A., Averill, B. A., & Tiedje, J. M. (1989) *Appl. Environ. Microbiol. 55*, 2924–2931.

Denariaz, G., Payne, W. J., & LeGall, J. (1991) *Biochim. Biophys. Acta 1056*, 225–232.

Farnden, K. J. F., & Robertson, J. G. (1980) in *Methods for Evaluating Biological Nitrogen Fixation* (Bergersen, F. J., Ed.) pp 265–314, J. Wiley and Sons, New York.

Feigin, L. A., & Svergun, D. I. (1987) *Structure Analysis by Small-Angle X-ray and Neutron Scattering*, pp 59–105, Plenum Press, New York.

Gerritsen, H. C., & Robertus, C. (1990) in *Applications of Synchrotron Radiation* (Catlow, C. R., & Greaves, G. N., Eds.) pp 100–120, Blackie & Sons, Glasgow.

Glatter, O. (1982) in *Small Angle X-ray Scattering* (Glatter, O., & Kratky, O., Eds.) pp 167–196, Academic Press, London.

Godden, J. W., Turley, S., Teller, D. C., Adman, E. T., Liu, M. Y., Payne, W. J., & LeGall, J. (1991) *Science 253*, 438–442.

Grossmann, J. G., Neu, M., Pantos, E., Schwab, F. J., Evans, R. W., Townes-Andrews, E., Lindley, P. F., Appel, H., Thies, W.-G., & Hasnain, S. S. (1992) *J. Mol. Biol. 225*, 811–819.

Grossmann, J. G., Neu, M., Evans, R. W., Lindley, P. F., Appel, H., & Hasnain, S. S. (1993) *J. Mol. Biol. 229*, 585–590.
Guinier, A. (1939) *Ann. Phys. 12*, 161–237.
Harding, S. E., Horton, J. C., & Morgan, P. J. (1993) in *Analytical Ultracentrifugation in Biochemistry and Polymer Sciences* (Harding, S. E., Horton, J. C., & Rowe, A. J., Eds.) Chapter 15, Royal Society of Chemistry, Cambridge (in press).
Hochstein, L.I., & Tomlinson, G. A. (1989) *Annu. Rev. Microbiol. 42*, 231–261.
Iwasaki, H. (1976) *Seikagaku 48*, 83–95.
Iwasaki, H., & Matsubara, T. (1972) *J. Biochem. 71*, 645–652.
Iwasaki, H., Shidara, S., Suzuki, H., & Mori, T. (1963) *J. Biochem. 53*, 299–303.
Konig, S., Svergun, D., Koch, M. H. J., Hubner, G., & Schellenberger, A. (1992) *Biochemistry 31*, 8726–8731.
Lewis, R., Sumner, I., Berry, A., Bordas, A., Bordas, J., Gabriel, A., Mant, G., Parker, B., Roberts, K., & Worgan, J. (1988) *Nucl. Instrum. Methods Phys. Res. A732*, 773–777.
Libby, E., & Averill, A. (1992) *Biochem. Biophys. Res. Commun. 187*, 1529–1535.
Liu, M.-Y., Liu, M.-C., Payne, W. J., & LeGall, J. (1986) *J. Bacteriol. 166*, 604–608.
MacGregor, C. H. (1978) *Methods Enzymol. 58*, 347–355.
Masuko, M., Iwasaki, H., Sakurai, T., Suzuki, S., & Nakahara, A. (1984) *J. Biochem. 96*, 447–454.
Mattevi, A., Obmolova, G., Schulze, E., Kalk, K. H., Westphal, A. H., Dekok, A., & Hol, W. G. J. (1992) *Science 255*, 1544–1550.
Rolbin, O. A., Kayushina, R. L., Feigin, L. A., & Shchedrin, B. M. (1974) *Sov. Phys.—Crystallogr. 18*, 442–444.
Rupley, J. A., Gratton, E., & Careri, G. (1983) *Trends Biochem. Sci. 8*, 18–22.
Semenyuk, A. V., & Svergun, D. I. (1991) *J. Appl. Crystallogr. 24*, 537–540.
Svergun, D. I., Semenyuk, A. V., & Feigin, F. A. (1988) *Acta Crystallogr. A44*, 244–250.